



# Correlation between infrared, THz and microwave dielectric properties of vanadium doped antiferroelectric $\text{BiNbO}_4$

Stanislav Kamba <sup>a,\*</sup>, Hong Wang <sup>b</sup>, Milan Berta <sup>a</sup>, Filip Kadlec <sup>a</sup>,  
Jan Petzelt <sup>a</sup>, Di Zhou <sup>b</sup>, Xi Yao <sup>b</sup>

<sup>a</sup> Institute of Physics, Academy of Sciences of the Czech Republic, Na Slovance 2, 18221 Prague 8, Czech Republic

<sup>b</sup> Electronic Materials Research Laboratory, Xi'an Jiaotong University, China

Available online 13 March 2006

## Abstract

Terahertz (THz) transmissivity and infrared (IR) reflectivity spectra of orthorhombic microwave (MW) ceramics  $\text{Bi}(\text{Nb}_{1-x}\text{V}_x)\text{O}_4$  ( $0.002 < x < 0.032$ ) were measured between 4 and  $3000\text{ cm}^{-1}$  (0.09–90 THz) at room temperature. A well underdamped mode, presumably the ferroelectric soft mode, was observed at  $25\text{ cm}^{-1}$ . Complex permittivity spectra obtained from the fits to our data were extrapolated down to the MW range and compared with the dielectric data near 5 GHz. The linear extrapolation of dielectric losses from THz down to the MW range is in agreement with the experimental MW losses. Addition of 3.2% of vanadium reduces the sintering temperature to  $850^\circ\text{C}$  and the dielectric properties ( $\epsilon' = 42.2$ ,  $Q \cdot f = 14,000\text{ GHz}$ ,  $\tau_f = +10\text{ ppm}/^\circ\text{C}$ ) remain at a level satisfactory for MW applications. Somewhat lower MW losses were observed in a sample sintered in the  $\text{N}_2$  atmosphere.

© 2006 Elsevier Ltd. All rights reserved.

**Keywords:** Sintering; Spectroscopy; Dielectric properties; Insulators; Microwave resonators

## 1. Introduction

Modern wireless communication systems moved to the microwave (MW) frequency region in the last decade. This technique uses ceramic dielectric resonators and filters with a high relative permittivity  $\epsilon'$ , high quality factor  $Q = \epsilon'/\epsilon''$  (i.e., low dielectric loss  $\epsilon''$ ) and a small or zero temperature coefficient  $\tau_f$  of the resonant frequency. However, most of the commercial MW dielectric materials require high sintering temperatures, therefore they are not compatible with silver or copper electrodes. With a view to applying the multilayer technology, development of new low-temperature-cofired ceramics (LTCC) with a sintering temperature lower than  $1000^\circ\text{C}$  has become a major issue.

Orthorhombic  $\text{BiNbO}_4$  is a good candidate for LTCC ceramics, because it can be prepared at temperatures between 900 and  $970^\circ\text{C}$ <sup>1</sup> and, at the same time, it shows reasonable dielectric properties ( $\epsilon' \approx 43$ ,  $Q \cdot f \approx 17,000\text{ GHz}$ , and  $\tau_f$  can be tuned to zero using various dopants).<sup>2</sup> An irreversible structural transi-

tion to a triclinic structure occurs if the ceramic is heated above  $1020^\circ\text{C}$ .<sup>3</sup> Orthorhombic  $\text{BiNbO}_4$  is antiferroelectric at room temperature, but becomes ferroelectric at  $360^\circ\text{C}$  and paraelectric at  $570^\circ\text{C}$ .<sup>4,5</sup>  $\text{BiNbO}_4$  has the same structure as the mineral stibiotantalite  $(\text{Sb}_{0.9}\text{Bi}_{0.1})(\text{Ta}_{0.84}\text{Nb}_{0.16})\text{O}_4$  and crystallizes in the orthorhombic space group  $Pnma$  ( $D_{2h}^{16}$ ) with 4 formula units per unit cell.<sup>6</sup> The structure can be viewed as a pseudo-layered structure in which layers of corner sharing  $\text{NbO}_6$  octahedra are separated along the  $b$ -axis by Bi atoms.<sup>6</sup> The sintering temperature can be further reduced by various additives like  $\text{V}_2\text{O}_5$ ,<sup>7,8</sup>  $\text{CuO}$ ,<sup>9,10</sup>  $\text{CeO}_2$ ,<sup>11</sup>  $\text{B}_2\text{O}_3$ ,<sup>12</sup>  $\text{ZnO}$ <sup>13</sup> or  $\text{Sb}_2\text{O}_5$ .<sup>14</sup> In the last case a sintering temperature as low as  $820^\circ\text{C}$  was reached. Valant and Suvorov<sup>15</sup> have shown that unfortunately  $\text{BiNbO}_4$  reacts with silver electrodes but much cheaper copper electrodes can be used.

Lattice dynamics of  $\text{BiNbO}_4$  ceramics was investigated using Raman and infrared (IR) spectroscopy by Ayyub et al.<sup>5,16</sup> IR transmission spectra were taken from the  $\text{BiNbO}_4$  powder dispersed in KBr (above  $400\text{ cm}^{-1}$ ) and in polyethylene (between 20 and  $180\text{ cm}^{-1}$ ) pellets. Factor-group analysis of the optic phonons in the orthorhombic phase yields  $\Gamma_{\text{opt}} = 8\text{A}_g(x^2) + 8\text{A}_u(-) + 9\text{B}_{1g}(xy) + 8\text{B}_{1u}(z) + 10\text{B}_{2g}(xz) + 9\text{B}_{2u}(y) + 9\text{B}_{3g}(yz) + 8\text{B}_{3u}(x)$  which means that 36 modes can be expected in

\* Corresponding author. Tel.: +420 266 052 957; fax: +420 286 890 527.

E-mail address: kamba@fzu.cz (S. Kamba).

Raman spectra, 25 modes should be IR active and 8 modes are silent (Raman and IR inactive). Ayyub et al. observed 19 modes in Raman and 21 modes in IR spectra. Raman spectra did not show any difference between 150 and 300 K. It means that the crystal structure probably does not change between these temperatures.

Our IR reflectivity and time-domain THz transmission studies of bulk BiNbO<sub>4</sub> ceramics allow us to determine the complex dielectric response between 4 and 3000 cm<sup>-1</sup> and correlate it with the MW dielectric response. It is well-established that the MW permittivity in materials with  $\epsilon' \leq 100$  is determined mainly by contributions of polar optic phonons and that the intrinsic dielectric loss should be in most cases proportional to the frequency between MW and THz range.<sup>17</sup> This allows us to determine if there is some extrinsic contribution to MW losses in our ceramics, i.e., if one could improve the sample processing to obtain lower MW losses.

## 2. Experimental

A set of Bi(Nb<sub>1-x</sub>V<sub>x</sub>)O<sub>4</sub> ceramics with various amount of vanadium was prepared (see Table 1). The sample processing was described in detail in ref.<sup>8</sup> The sintering was performed under ambient atmosphere. All the samples had densities higher than 95% of the theoretical value (7.35 g/cm<sup>3</sup>). The  $\epsilon'$  and  $Q$ -values are not significantly influenced by vanadium addition. The  $x=0.004$  sample has somewhat lower value of  $\epsilon'$  due to its lower density. It is seen that the addition of 3.2% of vanadium reduces the sintering temperature to 850 °C and the MW properties and density remain almost the same. The XRD pattern confirmed the orthorhombic structure of all the samples (see Fig. 1).

The MW dielectric properties at room temperature were measured using an 8720ES Network Analyzer at approximately 5 GHz using Hakki–Colemann method for measuring the TE<sub>018</sub> modes. The  $\tau_f$  values were measured by putting the cylindrical samples in a TE<sub>018</sub> cylindrical resonant cavity into a Delta 9023 temperature chamber.

Time-domain THz spectroscopy measurements were performed in the transmission mode using an amplified femtosecond laser system; two identical 1 mm thick [1 1 0] ZnTe single crystals were used to generate (by optic rectification) and detect (by electro-optic sampling) the THz pulses. Other details of the setup are described elsewhere.<sup>18</sup> Our THz technique allows the determination of the complex dielectric response,  $\epsilon^*(\omega) = \epsilon'(\omega) - i\epsilon''(\omega)$ , in the range from 3 to 80 cm<sup>-1</sup>

Table 1  
Microwave dielectric properties of Bi(Nb<sub>1-x</sub>V<sub>x</sub>)O<sub>4</sub> ceramics

$x$	$\epsilon'$	$Q$	$f$ (GHz)	Sintering temperature (°C)	$\tau_f$ (ppm/°C)	Density (g/cm <sup>3</sup> )
0.002	41.8	2964	4.892	990	+14	7.17
0.004	39.3	3233	5.394	910	+10	7.05
0.008	42.6	2456	4.918	890	+5	7.09
0.032	42.2	2777	4.923	850	+10	7.10

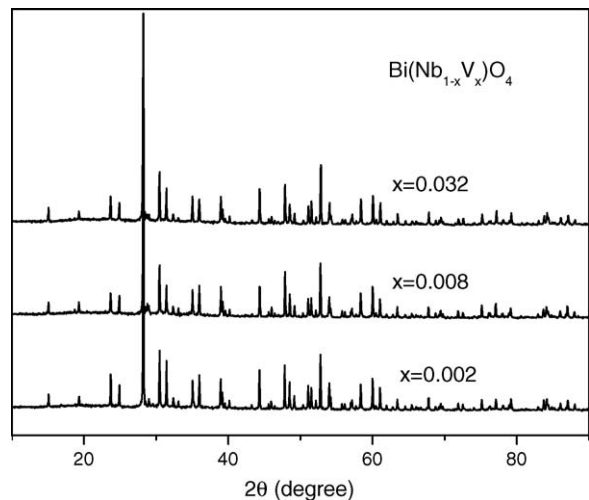


Fig. 1. X-ray diffraction patterns of Bi(Nb<sub>1-x</sub>V<sub>x</sub>)O<sub>4</sub> ceramics confirming the orthorhombic structure.

(0.1–2.4 THz); the useful spectral range depends on the transmissivity of the samples investigated.

Near-normal incidence IR reflectivity spectra at room temperature were obtained using a Fourier transform infrared (FTIR) spectrometer, Bruker IFS 113v, in the frequency range of 30–3000 cm<sup>-1</sup> (0.9–90 THz). The spectra were fitted together with the complex permittivity  $\epsilon^*(\omega)$  spectra in the THz range using a sum of damped harmonic oscillators

$$\epsilon^*(\omega) = \sum_{j=1}^n \frac{\Delta\epsilon_j \omega_j^2}{\omega_j^2 - \omega^2 + i\omega\gamma_j} + \epsilon_\infty \quad (1)$$

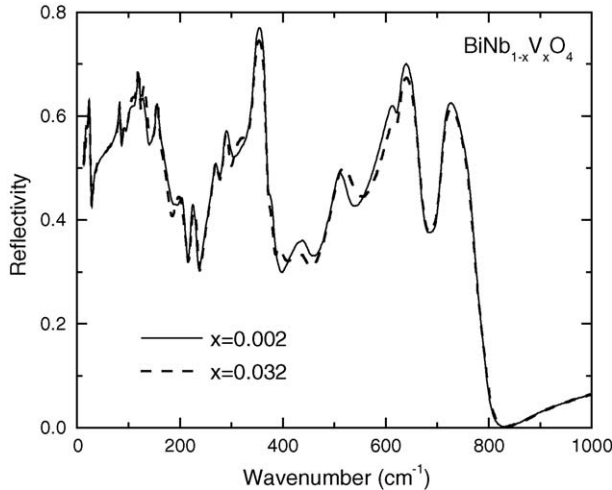
where  $\epsilon^*(\omega)$  is related to reflectivity,  $R(\omega)$ , by

$$R(\omega) = \left| \frac{\sqrt{\epsilon^*(\omega)} - 1}{\sqrt{\epsilon^*(\omega)} + 1} \right|^2. \quad (2)$$

$\omega_j$ ,  $\gamma_j$  and  $\Delta\epsilon_j$  are the frequency, damping and dielectric strength of the  $j$ -th mode, respectively. The high-frequency permittivity  $\epsilon_\infty$  results from electronic absorption processes much above the phonon frequencies (typically in the UV-vis range).

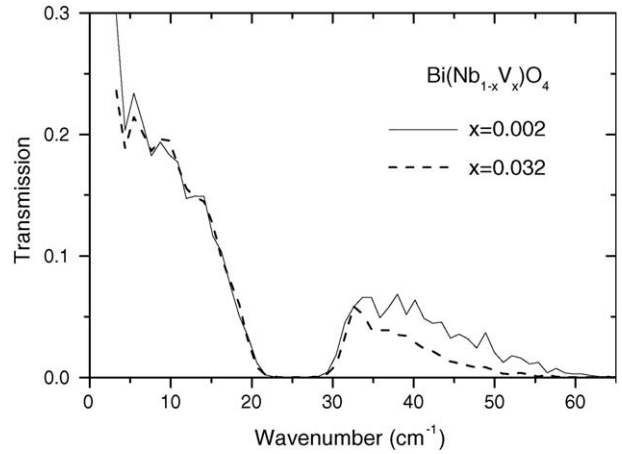
## 3. Results and discussion

Fig. 2 shows the FTIR reflectivity spectra of two Bi(Nb<sub>1-x</sub>V<sub>x</sub>)O<sub>4</sub> samples with the lowest and highest amount of vanadium. Most of the phonons display a low damping, indicating a highly ordered structure. The spectra are only slightly influenced by the vanadium, mainly in the range near 400 cm<sup>-1</sup>; some of the modes are more damped in the more doped sample. THz transmission spectra are shown in Fig. 3. A well pronounced transmission minimum is seen between 20 and 30 cm<sup>-1</sup> due to resonant phonon absorption. The same mode is seen also in the IR reflectivity (Fig. 2) as a sharp reflection band. Note that the phonon frequency at 25 cm<sup>-1</sup> is unusually low so that it could be the ferroelectric soft mode responsible for the ferroelectric phase transition at 570 °C. High temperature FTIR and THz experiments are needed to confirm this assumption. The time-domain

Fig. 2. Room temperature IR reflectivity spectra of  $\text{Bi}(\text{Nb}_{1-x}\text{V}_x)\text{O}_4$  ceramics.

THz spectra of the complex transmission (transmitted amplitude and phase shift) were evaluated and the complex permittivity spectra were calculated; see Fig. 4. However, due to the ambiguous determination of the phase shift above  $30 \text{ cm}^{-1}$ , the THz permittivity  $\epsilon'$  spectra in Fig. 4 are presented only below  $20 \text{ cm}^{-1}$ .

The reflectivity spectra were fitted together with the THz spectra using Eqs. (1) and (2) and the resulting mode parameters are listed in Table 2. We detected the same number of IR active phonons as predicted by the factor-group analysis. Our reflectivity spectra are more sensitive than the transmission spectra of powder published in ref. <sup>16</sup>, therefore, we observed higher number of modes. The modes which were not observed in ref. <sup>16</sup> are marked in Table 2 by bold numbers. The complex dielectric spectra obtained from the oscillator fit (Eq. (1)) are shown together with experimental THz and MW data in Fig. 4. A very

Fig. 3. Transmission spectrum of  $\text{Bi}(\text{Nb}_{1-x}\text{V}_x)\text{O}_4$  ceramics obtained by time-domain THz spectroscopy. Thickness of the samples was  $352 \mu\text{m}$ .

good agreement between the calculated  $\epsilon'$  spectra and the THz data was obtained; the correspondence is worse in the case of dielectric loss  $\epsilon''$  spectra, mainly due to an inaccuracy in the phase-shift determination.

Extrapolation of  $\epsilon'$  and  $\epsilon''$  from THz down to the MW range shows an agreement between the theoretical curves and experimental data within the accuracy of measurements. Because the IR and THz dielectric response is caused mostly by intrinsic processes (phonon absorption), the extrapolation of  $\epsilon^*$  down to the MW range determines mostly intrinsic MW  $\epsilon^*$ . Therefore, the MW complex permittivity is predominantly due to intrinsic processes, i.e., by difference two-phonon absorption, and the extrinsic contributions to dielectric losses are low. However, it was shown in ref. <sup>8</sup> that the sintering of  $\text{Bi}(\text{Nb}_{1-x}\text{V}_x)\text{O}_4$  ceramics under  $\text{N}_2$  atmosphere can improve the quality  $Q$  almost by a

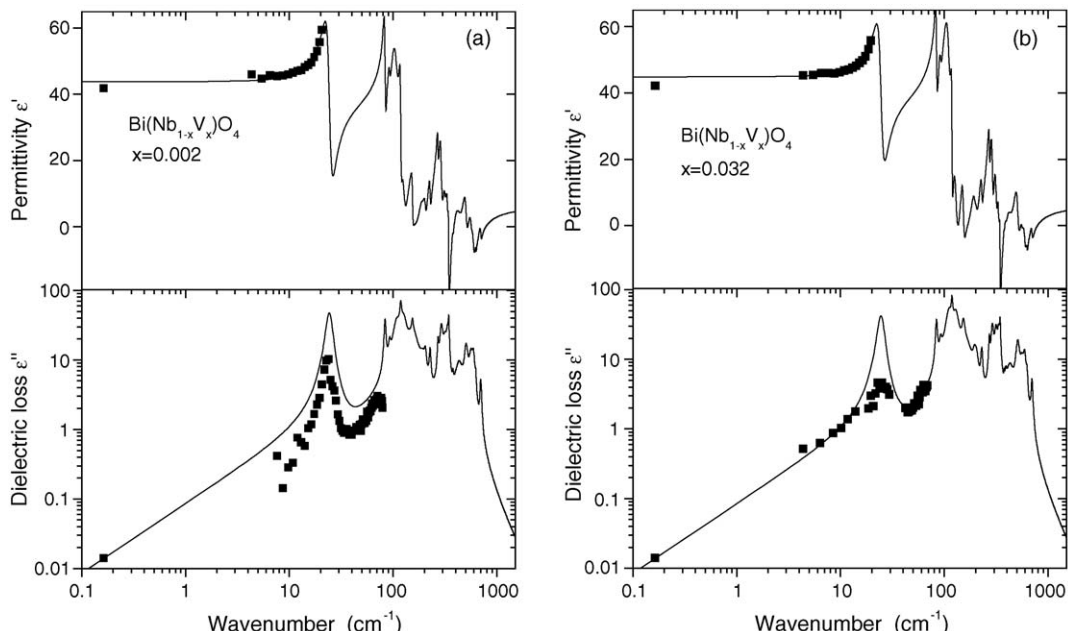
Fig. 4. Complex dielectric spectra of  $\text{Bi}(\text{Nb}_{1-x}\text{V}_x)\text{O}_4$  ceramics with (a)  $x=0.002$  and (b)  $x=0.032$ . Full symbols are experimental MW and THz data, solid lines are the results of the fits of IR and THz spectra.

Table 2

Phonon parameters obtained from the fit of IR and THz spectra

$x=0.002$				$x=0.032$			
Mod no.	$\omega_j$	$\Delta\epsilon_j$	$\gamma_j$	Mod no.	$\omega_j$	$\Delta\epsilon_j$	$\gamma_j$
1	24.4	8.0	4.2	1	24.6	7.5	4.4
2	83.6	1.4	3.7	2	83.8	1.3	3.7
<b>3</b>	92.6	0.4	4.9	3	92.1	0.5	5.9
<b>4</b>	107.1	1.1	14.6	4	109.9	4.4	22.9
<b>5</b>	110.0	4.0	22.2	5	110.8	2.4	13.7
6	118.6	1.4	4.8	6	118.3	1.5	4.4
7	126.7	4.2	19.0	7	129.2	5.2	18.8
<b>8</b>	153.7	0.5	6.4	8	152.5	1.3	10.5
9	157.0	6.1	45.4	9	163.0	4.3	51.6
10	193.0	0.7	25.3	10	195.7	0.6	17.5
11	204.2	0.4	11.3	11	204.7	0.4	15.0
12	227.2	0.4	9.3	12	228.9	0.4	10.1
<b>13</b>	270.9	0.4	9.1	13	270.8	0.5	9.6
14	291.7	2.0	21.6	14	289.8	1.5	16.8
<b>15</b>	316.7	1.5	29.4	15	314.1	1.7	23.3
16	333.4	0.8	16.6	16	332.0	0.8	16.0
17	343.9	0.8	9.2	17	343.6	0.9	10.6
18	377.0	0.0	7.9	18	376.6	0.0	5.7
			19		391.2	0.1	18.9
19	432.5	1.3	78.2	20	429.0	1.1	73.1
<b>20</b>	505.9	1.1	43.1	21	509.1	1.2	47.2
<b>21</b>	563.7	0.9	52.0	23	557.4	0.5	45.6
23	595.2	0.5	35.1	23	593.1	0.8	45.7
23	625.2	0.1	16.3	24	624.0	0.1	18.9
24	699.3	0.2	26.6	25	697.5	0.2	29.7

Phonon frequencies  $\omega_j$  and damping constants  $\gamma_j$  are in  $\text{cm}^{-1}$ , dielectric strengths  $\Delta\epsilon_j$  are dimensionless. The modes which were not observed in ref. <sup>16</sup> are marked by bold numbers.

factor of two ( $Q \cdot f = 28.5 \text{ THz}$ ) in comparison with our  $Q$ -values. It means that the intrinsic losses are lower still. It should be stated that the accuracy of our complex permittivity extrapolation from IR and THz range is limited and is sensitive only to strong processes in the IR-THz range. For example, uncorrelated charged point defects activate the acoustic phonon branches which contribute to dielectric losses with the same frequency dependence as the intrinsic losses (i.e.,  $\Delta\epsilon'' \propto \omega$ ),<sup>19</sup> but can only just be revealed in the THz and IR spectra. It was actually shown<sup>8</sup> that the oxygen vacancies play the main role in extrinsic contributions to the MW dielectric loss.

Temperature-dependent measurements of MW losses can provide more information about the origin of dielectric losses.<sup>20</sup> Fig. 5 shows temperature dependences of  $\epsilon'$  and  $Q$  measured near 5 GHz for the sample with the lowest concentration of vanadium. Theoretical predictions,<sup>19,21</sup> based on anharmonic interaction of an ac electric field with the phonon system of the crystal, lead to a quadratic (or even steeper) temperature dependence of the dielectric losses. The permittivity is only slightly temperature-dependent in MW ceramics (determined by temperature coefficient of permittivity  $\text{TC}\epsilon$ ), therefore one can expect a fast increase of  $Q$  on cooling ( $Q \sim 1/T^n$ ,  $n \geq 2$ ). However, Fig. 5 shows a decrease of  $Q$  on cooling, reaching a minimum near 170 K and only at lower  $T$  an increase in  $Q$  is seen. The minimum in  $Q(T)$  can be interpreted as due to slowing down of a dielectric relaxation on cooling, which passes through the mea-

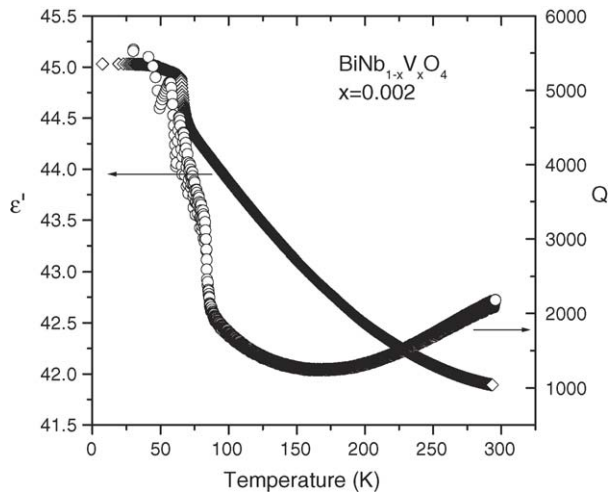


Fig. 5. Temperature dependences of permittivity  $\epsilon'$  and  $Q$  factor in  $\text{BiNb}_{1-x}\text{V}_x\text{O}_4$  ( $x=0.002$ ) measured near 5 GHz.

suring frequency of 5 GHz near 170 K and further decreases on cooling. When the dielectric relaxation slows down sufficiently, it no longer contributes to MW loss at 5 GHz and  $Q$  begins to increase dramatically, being determined predominantly by the intrinsic losses. Fig. 5 shows also another interesting fact; as soon as the dielectric relaxation slows down below 5 GHz, the MW permittivity below 70 K levels off. This can mean that the non-zero  $\text{TC}\epsilon$  (and also  $\tau_f$ ) above 100 K is mostly due to the relaxational contribution. This contribution could be of extrinsic origin so that there is a chance that with further improving the processing not only  $Q$  but also  $\tau_f$  could be improved. However, there is also another possible explanation for the knee in permittivity near 70 K. The shape of the dielectric anomaly could also be caused by a new structural phase transition. This possibility needs further investigation.

#### 4. Conclusion

A set of  $\text{Bi}(\text{Nb}_{1-x}\text{V}_x)\text{O}_4$  ceramics was prepared and studied by means of FTIR and THz spectroscopy and in the MW range. It was shown that while vanadium addition reduces the sintering temperature from 990 to 850 °C, the MW dielectric properties remain almost unchanged. The low sintering temperature and good MW parameters ( $\epsilon'=42.2$ ,  $Q \cdot f = 14,000 \text{ GHz}$ ,  $\tau_f = +10 \text{ ppm}/^\circ\text{C}$ ) makes the  $\text{Bi}(\text{Nb}_{0.968}\text{V}_{0.032})\text{O}_4$  ceramics promising as low-temperature cofired ceramics for MW applications. IR reflectivity spectra revealed all IR active phonons predicted by the factor-group analysis. A low-frequency mode was observed at  $25 \text{ cm}^{-1}$  and tentatively assigned to the ferroelectric soft mode. Extrapolation of the complex permittivity spectra from IR-THz range down to MW region corresponds to the measured MW data. The low-temperature MW study revealed a weak dielectric relaxation, which slows down on cooling and crosses the measuring frequency of 5 GHz near 170 K. At lower temperatures intrinsic phonon losses dominate so that the quality rapidly improves and the permittivity levels off. The dielectric anomaly near 70 K is indicative of a structural phase transition, but its confirmation needs further studies.

## Acknowledgements

This work was supported by the Czech Academy of Sciences (project AVOZ10100520), Grant Agency of the Czech Republic (project No. 202/04/0993) and Ministry of Education of the Czech Republic (project COST OC 525.20/00) and the Ministry of Science and Technology of China (973-project 2002CB613302).

## References

1. Aurivillius, B., X-ray investigations on  $\text{BiNbO}_4$ ,  $\text{BiTaO}_4$  and  $\text{BiSbO}_4$ . *Ark. Kemi*, 1951, **3**, 153–161.
2. Kagata, H., Inoue, T., Kato, J. and Kameyama, I., Low-fire bismuth based dielectric ceramics for microwave use. *Jpn. J. Appl. Phys.*, 1992, **31**, 3152–3155.
3. Keve, E. T. and Skapski, A. C., The crystal structure of triclinic  $\beta$ - $\text{BiNbO}_4$ . *J. Solid State Chem.*, 1973, **8**, 159–163.
4. Popolitov, V. I., Lobechev, A. N. and Peskin, V. F., Antiferroelectrics, ferroelectrics and pyroelectrics of a stibiotantalite structure. *Ferroelectrics*, 1982, **40**, 9–16.
5. Ayyub Pushan, Palkar, V. R., Multani, M. S. and Vijayaraghavan, R., Structural, dielectric and vibrational properties of the stibiotantalite ( $\text{Sb}_{1-x}\text{Bi}_x\text{NbO}_4$ ) system for  $0 \leq x \leq 1$ . *Ferroelectrics*, 1987, **76**, 93–106.
6. Lee, Ch.-Y., Macquart, R., Zhou, Q. and Kennedy, B. J., Structural and spectroscopic studies of  $\text{BiTa}_{1-x}\text{Nb}_x\text{O}_4$ . *J. Solid State Chem.*, 2003, **174**, 310–318.
7. Tzou, W.-Ch., Yang, Ch.-F., Chen, Y.-Ch. and Cheng, P. S., Improvements in the sintering and microwave properties of  $\text{BiNbO}_4$  microwave ceramics by  $\text{V}_2\text{O}_5$  addition. *J. Eur. Ceram. Soc.*, 2000, **20**, 991–996.
8. Wang, Z., Yao, X. and Zhang, L., The effect of sintering atmosphere on the microwave dielectric properties of  $\text{V}_2\text{O}_5$  doped  $\text{BiNbO}_4$  ceramics. *Ceram. Int.*, 2004, **30**, 1929–1933.
9. Huang, Ch.-L. and Weng, M.-H., The microwave dielectric properties of the microstructures of  $\text{Bi}(\text{NbTa})\text{O}_4$  ceramics. *Jpn. J. Appl. Phys.*, 1999, **38**, 5949–5952.
10. Huang, Ch.-L., Weng, M.-H. and Yu, Ch.-Ch., Low-firable  $\text{BiNbO}_4$  based microwave dielectric ceramics. *Ceram. Int.*, 2001, **27**, 343–350.
11. Wang, Z., Yao, X. and Zhang, L.,  $\text{CeO}_2$ -modified  $\text{BiNbO}_4$  microwave ceramics sintered under atmosphere. *Ceram. Int.*, 2004, **30**, 1329–1333.
12. Ding, S., Yao, X. and Yang, Y., Dielectric properties of  $\text{B}_2\text{O}_3$ -doped  $\text{BiNbO}_4$  ceramics. *Ceram. Int.*, 2004, **30**, 1195–1198.
13. Yang, Y., Ding, S. and Yao, X., Study of the relationship between the defect and dielectric properties of  $\text{ZnO}$ -doped  $\text{BiNbO}_4$  ceramics. *Ceram. Int.*, 2004, **30**, 1335–1339.
14. Wang, N., Zhao, M.-Y., Li, W. and Yin, Z.-W., The sintering behavior and microwave dielectric properties of  $\text{Bi}(\text{NbSb})\text{O}_4$  ceramics. *Ceram. Int.*, 2004, **30**, 1017–1022.
15. Valant, M. and Suvorov, D., Chemical compatibility between silver electrodes and low-firing binary-oxide compounds: conceptual study. *J. Am. Cer. Soc.*, 2000, **83**, 2721–2729.
16. Ayyub Pushan, Multani, M. S., Palkar, V. R. and Vijayaraghavan, R., Vibrational spectroscopic study of ferroelectric  $\text{BiNbO}_4$ , antiferroelectric  $\text{BiNbO}_4$  and their solid solutions. *Phys. Rev. B*, 1986, **34**, 8137–8140.
17. Petzelt, J. and Kamba, S., Submillimetre and infrared response of microwave materials: extrapolation to microwave properties. *Mater. Chem. Phys.*, 2003, **79**, 175–180.
18. Kuzel, P. and Petzelt, J., *Ferroelectrics*, 2000, **239**, 949–956.
19. Petzelt, J. and Setter, N., Far infrared spectroscopy and origin of microwave losses in low-loss ceramics. *Ferroelectrics*, 1993, **150**, 89–102.
20. Kamba, S., Noujni, D., Pashkin, A., Petzelt, J., Pullar, R. C., Axelsson, A.-K. et al., Low-temperature microwave and THz dielectric response in novel microwave ceramics. *J. Eur. Ceram. Soc.*, 2006, **26**, 1845–1851.
21. Gurevich, V. L. and Tagantsev, A. K., Intrinsic dielectric loss in crystals. *Adv. Phys.*, 1991, **40**, 719–767.